



Wls-mediated Wnts differentially regulate distal limb patterning and tissue morphogenesis

Xuming Zhu^{a,b}, Huang Zhu^b, Lingling Zhang^b, Sixia Huang^b, Jingjing Cao^b, Gang Ma^b, Guoying Feng^b, Lin He^{a,b}, Yingzi Yang^c, Xizhi Guo^{b,*}

^a Institute for Nutritional Sciences, Shanghai Institutes for Biological Sciences, Chinese Academy of Sciences; Graduate School of the Chinese Academy of Sciences, China

^b Bio-X Institutes, Key Laboratory for the Genetics of Developmental and Neuropsychiatric Disorders, Shanghai Jiao Tong University, 200240, China

^c Developmental Genetics Section, National Human Genome Research Institute, NIH, 20892, USA

ARTICLE INFO

Article history:

Received for publication 6 December 2011

Revised 6 February 2012

Accepted 14 February 2012

Available online 22 February 2012

Keywords:

Wntless
Wnt
Limb
Patterning
Tissue morphogenesis
Tendon/ligament

ABSTRACT

Wnt proteins are diffusible morphogens that play multiple roles during vertebrate limb development. However, the complexity of Wnt signaling cascades and their overlapping expression prevent us from dissecting their function in limb patterning and tissue morphogenesis. Depletion of the *Wntless* (*Wls*) gene, which is required for the secretion of various Wnts, makes it possible to genetically dissect the overall effect of Wnts in limb development. In this study, the *Wls* gene was conditionally depleted in limb mesenchyme and ectoderm. The loss of mesenchymal *Wls* prevented the differentiation of distal mesenchyme and arrested limb outgrowth, most likely by affecting Wnt5a function. Meanwhile, the deletion of ectodermal *Wls* resulted in agenesis of distal limb tissue and premature regression of the distal mesenchyme. These observations suggested that Wnts from the two germ layers differentially regulate the pool of undifferentiated distal limb mesenchyme cells. Cellular behavior analysis revealed that ectodermal Wnts sustain mesenchymal cell proliferation and survival in a manner distinct from Fgf. Ectodermal Wnts were also shown for the first time to be essential for distal tendon/ligament induction, myoblast migration and dermis formation in the limb. These findings provide a comprehensive view of the role of Wnts in limb patterning and tissue morphogenesis.

© 2012 Elsevier Inc. All rights reserved.

Introduction

Vertebrate limb patterning and morphogenesis start from a limb bud consisting of multipotent mesenchyme and the overlying ectoderm. In the process of limb patterning, mesenchymal cells in the limb bud integrate positional information from the three axes. Fgf signal from the apical ectodermal ridge (AER) induces formation of the proximal–distal (PD) axis (Mariani et al., 2008), while the Shh signal from the zone of polarizing activity (ZPA) establishes anterior–posterior (AP) polarity (Mariani and Martin, 2003). To establish dorsoventral (DV) patterning, limb mesenchyme requires a *Wnt7a* signal from the dorsal ectoderm and an *En1* signal from the ventral ectoderm (Riddle et al., 1995). Among the many signals governing limb patterning, the role of AER-derived Fgf signaling in the regulation of PD patterning is particularly well recognized. AER-Fgf signaling acts as a timer to modulate the size of the pool of distal mesenchymal progenitor cells underneath the AER (Mariani et al., 2008; Sun et al., 2002; Yu and Ornitz, 2008). Fgf also serves as a distal signal that counteracts proximal Retinoic Acid (RA) signaling to fine-tune limb PD patterning (Cooper et al., 2011; Rosello-Diez et al.,

2011). AER-Fgf also forms a feedback loop with ZPA-Shh to regulate limb AP patterning and outgrowth (Scherz et al., 2004; Verheyden and Sun, 2008).

Although a large wealth of knowledge regarding the mechanisms controlling limb patterning has accumulated, the molecular network instructing limb morphogenesis is still not well defined. For instance, the limb skeletal elements and tendons are formed with mesenchyme that originates from the lateral plate mesoderm in somites, whereas muscle mass is derived from myoblasts that migrated from somite dermomyotome (Buckingham et al., 2003). The molecular mechanisms that determine how these processes are tightly coordinated during limb morphogenesis are beginning to be elucidated. Recent evidence has shown that Fgfs and Wnts coordinately maintain the undifferentiated pool of mesenchymal progenitors and specify the differentiation of distal limb mesenchyme into skeletal or soft connective tissue (ten Berge et al., 2008). Wnt signaling has also been reported to regulate myoblast migration and dermal cell specification (Geetha-Loganathan et al., 2005; Tran et al., 2011).

In the vertebrate limb, more than 15 members of the Wnt family are expressed dynamically and play redundant roles in limb development (Witte et al., 2009). As mentioned above, *Wnt7a* from the dorsal ectoderm not only dictates DV polarity through induction of *Lmx1b* expression in the underlying mesenchyme (Riddle et al., 1995) but also contributes to AP pattern formation (Yang and Niswander,

* Corresponding author at: #800 Dongchuan Road, Biomedical Building #1-205, Shanghai, 200240, China. Fax: +86 21 34206736.

E-mail address: xzguo2005@sjtu.edu.cn (X. Guo).

1995). In the chicken, Wnt2b-Wnt8c/ β -catenin signaling in the lateral plate mesoderm is required for *Fgf10* expression in the presumptive limb bud mesenchyme, mediating the *Fgf8/Fgf10* feedback loop in limb bud formation and AER maintenance (Kawakami et al., 2001). Genetic studies in mice revealed that ectodermal Wnt3/ β -catenin signaling establishes and maintains AER function (Barrow et al., 2003). Mesenchymal β -catenin signaling is also required for AER maintenance and mesenchyme survival (Hill et al., 2006). Meanwhile, Wnt5a also promotes limb outgrowth by establishing planar cell polarity (PCP) along the PD axis (Gao et al., 2011; Yamaguchi et al., 1999).

The Wnt protein family can be classified into canonical and non-canonical signaling pathways. Canonical Wnts, such as Wnt1/Wnt3, signal through the intracellular mediator β -catenin to activate downstream targets (Bejsovec, 2000). Non-canonical Wnts, such as Wnt5a/Wnt11, seem to act through PCP or Ca^{2+} cascades to fulfill their function. In genetic studies, single Wnt protein or β -catenin is usually individually manipulated to elucidate the function of Wnt signaling. However, the overlapping expression pattern of the various Wnts and their functional redundancy obscure the true consequences of removing individual *Wnt* genes. Meanwhile, β -catenin does play a central role in the canonical Wnt pathway, but it also serves as a membrane protein of the cell junction complex (Aberle et al., 1996), thus its genetic modification most likely affects additional functions independent of Wnt signaling.

Wls was first identified in the fruit fly and worm as a cargo protein that functions in Wnt ligand secretion (Port et al., 2008), and its conserved function is confirmed in several model organisms (Banziger et al., 2006; Kim et al., 2009). Blocking this gene by different methods causes various phenotypes corresponding to Wnt signaling failure (Adell et al., 2009; Kim et al., 2009). Recently, Wls was both conventionally and conditionally targeted to study the role of Wnts in mouse embryonic development (Fu et al., 2011, 2009). Thus, Wls conditional inactivation makes it possible to dissect the overall role of Wnts in limb patterning and tissue morphogenesis.

Here, we generated a Wls conditional knockout mouse line carrying an exon3-floxed allele. Removal of Wls by limb-mesenchyme-specific *Prx1-Cre* and ectoderm-specific *Msx2-Cre* showed that Wls-mediated Wnts regulate early patterning along the three axes of the limb bud and also sustain cell proliferation and survival of distal limb mesenchyme. However, the Wnts from the two germ layers exerted distinct effects on modulating the undifferentiated pool of mesenchymal progenitors. At later developmental stages, ectodermal Wnts, most likely canonical Wnts, were found to coordinate soft tissue specification, including tendon/ligament induction, myoblast migration and dermis formation.

Materials and methods

Mice and genotyping

Wls^{c/c} (C57BL/6) mice were crossed with transgenic mouse lines *Prx1-Cre* or *Msx2-Cre*. *Prx1^{cre/+}*; Wls^{c/+} or *Msx2^{cre/+}*; Wls^{c/+} offspring were backcrossed to Wls^{c/c} mice to generate the limb-specific knock-out mice *Prx1^{cre/+}*; Wls^{c/c} or *Msx2^{cre/+}*; Wls^{c/c}. The floxed status of the Wls conditional allele was genotyped with the primers: P1: 5'-ATACTTTTCTGATCTGTTGT-3' and P2: 5'-AAGTTTAATAGGTCTGTGTT-3'. The presence of *Msx2-Cre* was identified by PCR using the primers: F-5'-CAAAAGTTGGAGTCTTCGCT-3' and R-5'-CAGAAG CA TTTCCAGGT AT-3'. The primers for genotyping *Prx1-Cre* were F-5'-ACCTGAAGATGTTCCGATTATCT-3' and R-5'-ACCGTCAGTACGTGAGATATCTT-3'.

Mice were maintained in a specific pathogen-free environment, with free access to food and water and a 12-h/12-h light-dark cycle. Animal welfare and experimental procedures were carried out strictly

in accordance with the care and use of laboratory animals and the related ethical regulations of Shanghai Jiao Tong University.

Chicken embryo collection

Fertilized chicken eggs are incubated in 38 °C for the desired time, and embryos are staged as described previously (Hamburger and Hamilton, 1951).

RNA in situ hybridization

Whole-mount RNA in situ hybridizations were performed as previously described (Guo et al., 2004) using the probes for *Bmp4*, *Fgf8*, *Fgf10*, *Lmx1b*, *Msx1*, *Shh*, *Wnt5a*, *Hoxd13* (Yamaguchi et al., 1999); *Sox9*, *Dermo1*, *Lef1* and *Scleraxis* (Guo et al., 2004). *En-1* is kindly provided by Dr. A.L. Joyner. *Wnt7a* was amplified by the primers: F-5'-CACTGTCCTTGTCTTTTCTGCT-3 and R-5'-CCGCTCGAGACCCAGGCAT CTGGTAACTG-3. *Pax3* was generated by its complete coding sequence. The mouse Wls probe was prepared from a 450 bp fragment of cDNA (NM_026582) amplified by PCR with the primers: F-5'-ACCACTATAACCCATGTAGATG-3' and R-5'-ATCCCAGAATCAAAA GCAG-A-3'. A fragment cDNA (NM_001031294.1) of the unique chick homologue of Wls was amplified with the primers: F-5'-CTCCTTCTGTGCGACCTCAA-3' and R-5'-ATCTGCTGCCATACATCTG-3'.

RT-PCR

E12.5 *Prx1^{cre/+}*; Wls^{c/c} mouse embryos and their littermates were collected, their forelimbs amputated and as much ectoderm as possible peeled off using forceps. Total RNA was extracted from the tissue using Trizol reagent (Invitrogen, CA, USA). cDNA was reverse transcribed using SuperScript™ III First-Strand Synthesis System for RT-PCR (Invitrogen, CA, USA) and the primers F: 5'-ACCGTATGATATGTTTTCTG-3' and R: 5'-TACCACACCATAATGATGAA-3'. Genomic DNA was prepared from the yolk sac membrane of embryos or from the tail tips of pups.

Immunohistochemistry and Antibodies

Tissues were either frozen-sectioned or paraffin-sectioned, prepared as 10- μm -thick slices, and then stained with anti- β -catenin, anti-Wls (Santa Cruz, CA, USA), anti-Ki-67, anti-Myosin (Epitomics, CA, USA), anti-keratin5 (Covance, NJ, USA), and anti-BrdU (Sigma, MO, USA) primary antibodies or Alexa Fluor® 488 (Invitrogen, CA, USA) secondary antibody. All antibodies were used according to the recommended dilution ratio. Labeled sections were counterstained with DAPI fluorescent dye (Southern Biotech, AB, USA), observed using a Leica confocal microscope, and then photographed. LysoTracker Red-DND-99 (Molecular Probes, The Netherlands) and a TUNEL assay kit (Promega, WI, USA) were used to label apoptotic cells. Safranin O staining and LacZ staining were performed as previously described (Guo et al., 2004).

Skeletal analysis

Newborn mouse embryos at E16.5 or P0 were skinned, eviscerated, and fixed in 95% ethanol. Skeletal preparations were performed as previously described (Guo et al., 2004).

Luciferase assay

The mouse *Scleraxis* promoter region (−1,344 to −676) and the minimal promoter region (−344 to +126) were cloned into the pGL3-Basic vector (Promega, WI, USA). Site-directed mutagenesis was performed using the QuikChange® Lightning kit (Stratagen, Australia) to introduce mutations in the two presumed Lef1/Tcf1 binding

sites (–1156 to –1147; –742 to –733), which were replaced by ATGATGCACG. C3H10T1/2 cells were cultured in DMEM supplemented with 10% FBS. For each transfection, cells were plated in a 24-well plate and then transfected with 0.8 μ g of experimental vector and 10 ng of pRL-TK (Promega, WI, USA), the latter as an internal control. Transfections were carried out using FuGene 6 transfection reagent (Roche, Switzerland). Wnt3a-conditioned medium or L-cell supernatant was added to the cells at the time of transfection. After 48 hr of culture, the cells were harvested and a luciferase assay was performed using a dual luciferase reporter assay system and a GloMax 20/20 Luminometer (Promega, WI, USA).

Results

Wls is ubiquitously expressed in limb ectoderm and mesenchyme

The results of whole-mount *in situ* hybridization showed that the *Wls* gene was extensively expressed in mouse limb tissues from E9.5 to E13.5 (Figs. 1A–E). Immunohistochemical (IHC) examination of sections also indicated that *Wls* was expressed in limb ectoderm and mesenchyme at E10.5 (Fig. 1J). The chicken *Wls* homologue was also expressed in the distal wing bud (Supplemental Figs. S2A and B), indicating a conserved function of *Wls* in limb development in vertebrates. Meanwhile, *Lef1* and *Wnt5a* were expressed in a pattern similar to that of *Wls* at early stages of E9.5 and E10.5 (Figs. 1 F–I). *Lef1* is a reporter of canonical Wnt signaling activity, while *Wnt5a* is a representative non-canonical Wnt. These results imply that *Wls* may be involved in regulating limb development through mediating the functions of various Wnts.

Generation of *Wls* conditional knockout mice

To investigate the role of *Wls* in limb organogenesis, a mouse line carrying the conditional *Wls* allele with exon3 flanked by loxP sites was generated. Exon3 encodes the first transmembrane domain of *Wls* (Supplemental Fig. S1A). The conditional allele *Wls^{cl/c}* was identified by PCR using primer P1/P2 (Supplemental Fig. S1B). In the forelimb of the *Prx1^{cre/+}; Wls^{cl/c}* mutant, *Wls* expression was significantly reduced compared to wild type (Supplemental Fig. S1C). The decrease in *Wls* protein was also observed in the limb ectoderm of the *Msx2^{cre/+}; Wls^{cl/c}* mutant (Supplemental Fig. S1D). In line with previous findings (Fu et al., 2011; Yu et al., 2010), our data showed that deletion of exon3 was sufficient to block the expression of the *Wls* gene.

Deletion of limb mesenchymal *Wls* results in hypoplastic skeletons

To elucidate the role of mesenchymal Wnts in limb morphogenesis, *Wls* was first inactivated in *Prx1-Cre* transgenic mice, which have specific Cre activity in limb mesenchyme from the early stages of limb initiation (Logan et al., 2002). Most of the *Prx1^{cre/+}; Wls^{cl/c}* mutant mice died at the weaning stage due to a failure of food and water intake caused by the limb abnormality. The mutant limbs displayed hypoplastic and shortened skeletons with truncated autopods (Figs. 2A and A'). Skeletal preparations showed that the limb skeletons of *Prx1^{cre/+}; Wls^{cl/c}* mutant embryos were smaller than those of the wild type (Figs. 2B–C'). The limb defects were much more severe in the forelimbs than those of the hindlimbs because of the stronger Cre activity in the forelimbs. No obvious defect in limb patterning was detected except for the truncation of the autopods (Figs. 2C and C'). However, skeletal ossification, including cartilage hypertrophy and osteogenesis, was also delayed (data not shown).

Because *Wnt5a* is the major Wnt expressed in the early limb mesenchyme (Witte et al., 2009), we first compared the limb defects of the *Prx1^{cre/+}; Wls^{cl/c}* mutant embryos with those of the *Wnt5a^{-/-}* embryos. As expected, defects in the forelimb skeletons of *Prx1^{cre/+}; Wls^{cl/c}* mutant embryos phenocopied those of *Wnt5a^{-/-}* embryos (Figs. 2A' and A"; B' and B"). Previous evidence has shown that *Wls* is required for *Wnt5a* secretion in cell lines (Banziger et al., 2006); our results strongly suggest that *Wls* is critical for limb PD outgrowth by mediating the secretion and function of *Wnt5a* in the distal limb.

Distal limb mesenchymal differentiation is arrested without mesenchymal *Wls*

To understand the molecular mechanism underlying skeletal agenesis in *Prx1^{cre/+}; Wls^{cl/c}* mutant mice, limb patterning was assessed by whole-mount *in situ* hybridization. Early initiation and PD elongation of the limb bud were normal in *Prx1^{cre/+}; Wls^{cl/c}* mutants, as revealed by the normal expression of *Fgf8* (a marker of AER integrity and function) and *Fgf10* (a marker of distal mesenchyme progenitors) (Supplemental Figs. S3A–B'). No obvious molecular or morphological alteration in the limb bud was detected in either the *Prx1^{cre/+}; Wls^{cl/c}* or the *Wnt5a^{-/-}* mutant embryos before E11.5. However, in both mutants, digit rays had failed to extend distally, reflected by the confined expression of *Sox9* (a chondrocyte marker) at E12.5 (Figs. 3A and A'). Instead, a continuous ring of distal mesenchyme remained in both mutant limbs (marked by arrow in Fig. 3A'). However, these cells were arrested from further differentiation, as indicated by the strong expression of *Fgf10* and *Msx1* (Figs. 3B–C'), markers

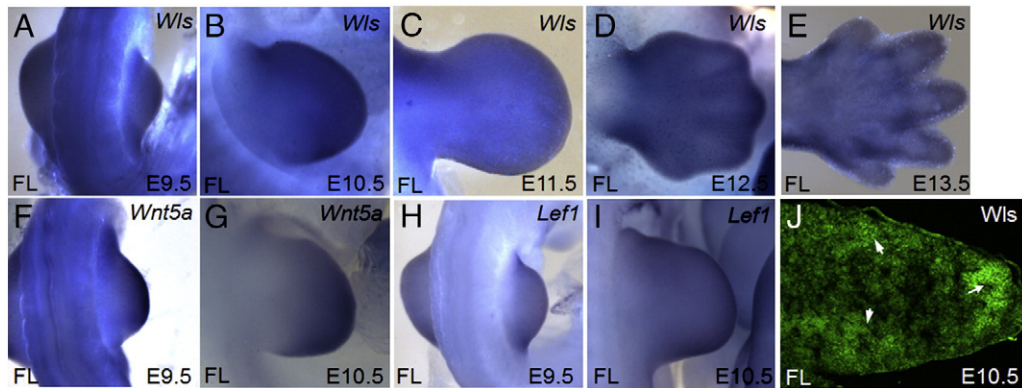


Fig. 1. *Wls* is ubiquitously expressed in the limb ectoderm and mesenchyme. (A and B) *Wls* is expressed in the entire limb bud of E9.5 and E10.5 stage embryos with a progressive proximal to distal gradient. The *Wls* expression pattern covers the expression region of *Wnt5a* (F and G) and *Lef1* (H and I). Expression of *Wls* ubiquitously persists in the limb from E11.5–E13.5 (C–E). (J) IHC shows *Wls* is extensively expressed in the distal mesenchyme of the forelimb at E10.5 (white arrow). Abbreviation: FL, forelimb.

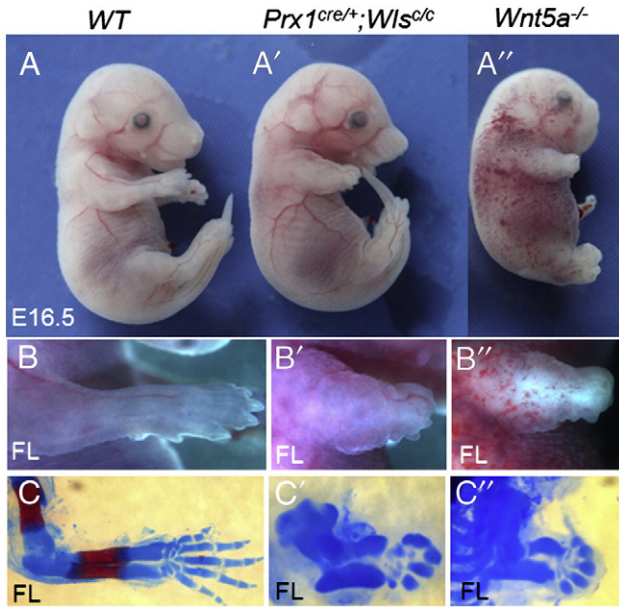


Fig. 2. The similar hypoplastic forelimb skeletons of *Prx1^{cre/+}; Wls^{cl/c}* and *Wnt5a^{-/-}* embryos at E16.5. (A–A'') Similar hypoplastic forelimbs and truncated autopods are detected in *Prx1^{cre/+}; Wls^{cl/c}* and *Wnt5a^{-/-}* mutant embryos. (B–B'') Magnification of the forelimbs in (A–A''). (C–C'') Skeletal preparation of forelimbs in (B–B''). Abbreviation: FL, forelimb.

for undifferentiated distal mesenchymal progenitors. These mesenchymal cells in the ring retained distal identity, as indicated by their expression of *Hoxd13*, an autopod progenitor marker (Figs. 3D and D'). However, they did not differentiate into other tissues, such as muscle, tendon/ligament or dermis, as they did not display changes in the expression of *Myf5*, *Dermo1* and *Scleraxis*, the marker of muscle, tendon progenitors and dermis respectively (Supplemental Fig. S5). The block in cell differentiation may have resulted from the elevated Wnt signaling activity in the distal mesenchyme, reflected by the higher level of β -catenin in the distal tip of mesenchymal *Wls* null mutants (arrows in Figs. 3E and E'). The elevated β -catenin level in the distal mesenchyme was also detected in the *Wnt5a^{-/-}* embryo

(arrow in Fig. 3E''). It is in line with previous findings that loss of *Wnt5a* could lead to increased canonical Wnt activity and inhibited differentiation of distal mesenchyme (ten Berge et al., 2008; Topol et al., 2003). Taken together, these results indicate that the inactivation of limb mesenchymal *Wls* arrests distal mesenchymal differentiation, most likely due to the blocking of *Wnt5a* secretion.

Distal limb agenesis upon depletion of ectodermal Wls

To dissect the comprehensive function of Wnts as diffusible morphogens in limb development, *Wls* was also specifically deleted in limb ectoderm by crossing *Wls^{cl/c}* mice with *Msx2-Cre* mice, which express ventral ectoderm and AER-specific *Cre* (Sun et al., 2002). *Msx2^{cre/+}; Wls^{cl/c}* mutant mice exhibit truncated limbs at the level of autopod in all limbs, but hindlimb also have shortened zeugopod (Figs. 4D–E''). Both the fore- and hindlimbs in the mutant were dorsally flexed (Figs. 4B–C'). The defects in the hindlimbs are more severe than in the forelimbs (shortened fibula and tibia as arrows in Figs. 4E' and E''), most likely due to earlier and broader *Cre* activity in the hindlimb (Barrow et al., 2003; Sun et al., 2002). In addition, *Msx2-Cre* mice displayed *Cre* activity in the skull, as indicated by LacZ staining in *Msx2^{cre/+}; R26R* reporter mice (Fig. 4F). The inhibition of *Wls* expression in the *Msx2^{cre/+}; Wls^{cl/c}* mutant had deleterious effects on suture fusion and intramembranous ossification in the skull (arrows in Figs. 4G and G'), matching phenotypes in *Wnt9a^{-/-}* mice (Spater et al., 2006).

Impairment of limb patterning with loss of ectodermal Wls

We first examined *Wls* expression in the *Msx2^{cre/+}; Wls^{cl/c}* mutant embryo at E12.5. IHC results indicated *Wls* protein expression was markedly decreased in the mutant forelimb ectoderm and in the underlying mesenchyme (Supplemental Fig. S1D). The decrease in dorsal ectoderm was milder due to weak *Cre* activity. As expected, ectodermal deletion of *Wls* significantly down-regulated canonical Wnt signaling activity, which was indicated by decreased *Lef1* expression at the distal tip (arrows in Figs. 5A and A'). The AER structure, evaluated by the expression of *Fgf8*, became thinner and narrower in the *Msx2^{cre/+}; Wls^{cl/c}* embryo than in the control at E10.5 (Figs. 5B

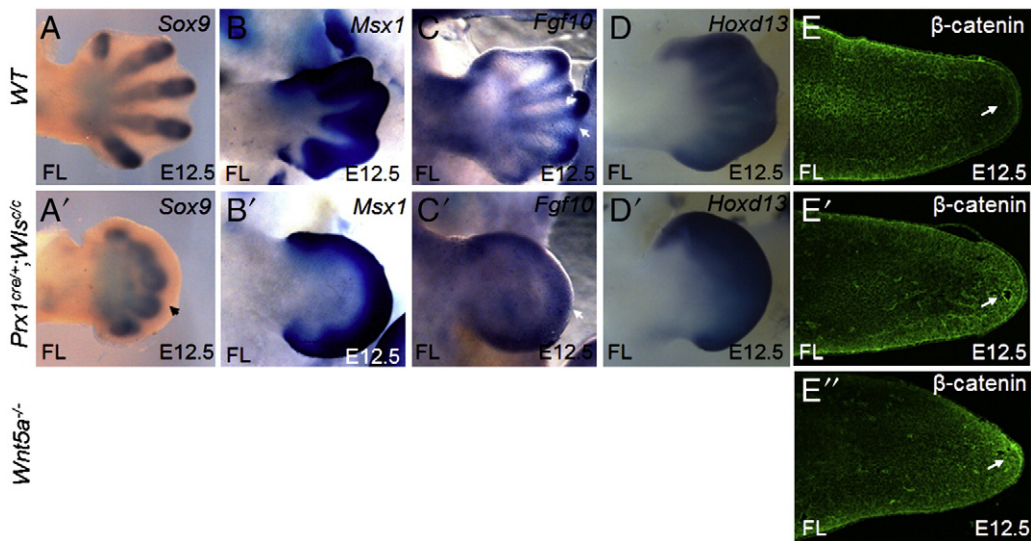


Fig. 3. Distal limb mesenchyme differentiation is arrested in the *Prx1^{cre/+}; Wls^{cl/c}* mutant at E12.5. (A–A') *Sox9* expression is excluded from the distal tip of the *Prx1^{cre/+}; Wls^{cl/c}* mutant forelimb. (B–D') Expression of the progenitor markers *Msx1* (B–B'), *Fgf10* (C–C', white arrows) and the autopod marker *Hoxd13* (D and D') remains at high level in the distal limbs of the mutant. (E–E'') An elevated β -catenin level is observed in the distal mesenchyme in the mutant without mesenchymal *Wls* and *Wnt5a* (white arrows) compared to wild type. Abbreviation: FL, forelimb.

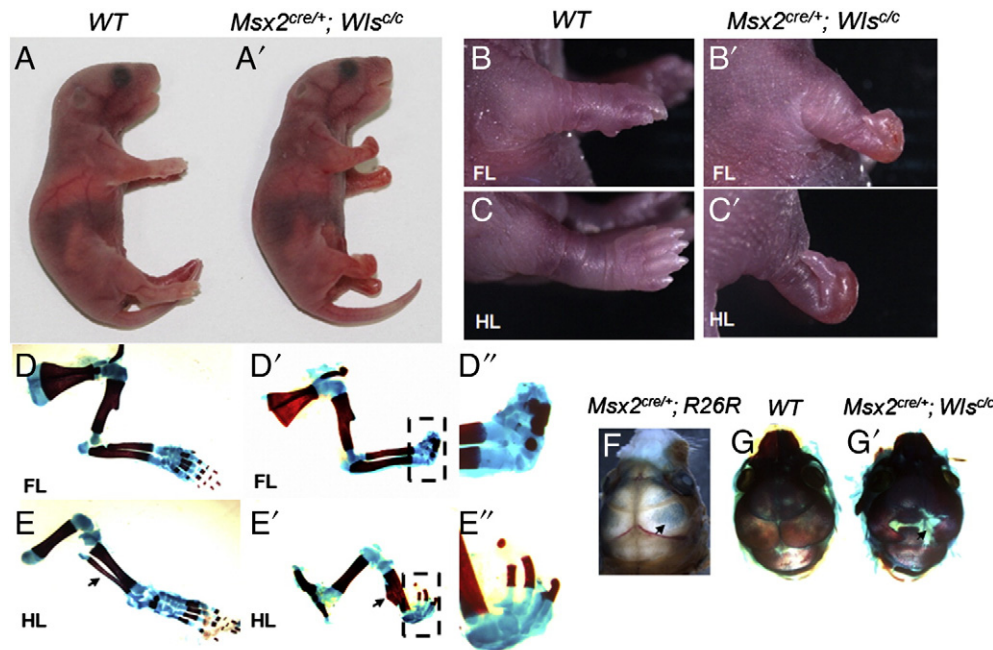


Fig. 4. Abnormal limbs in the *Msx2^{cre/+}; Wls^{c/c}* mutant. (A and A') Perinatal lethal *Msx2^{cre/+}; Wls^{c/c}* mutant embryo at P0. (B and B') Magnified view of the forelimbs. The mutant forelimb is shorter and autopod is dorsally flexed. (C and C') Magnified view of the hindlimbs, the defects of the mutant hindlimb show similarity with that of forelimb, but display a greater severity. (D–E') Skeleton staining of limbs in B–C'. The mutant forelimb has a relatively normal stylopod and zeugopod but an abnormal autopod; while the mutant hindlimb phenotype also extends to the zeugopod, especially the fibula (black arrowhead). (D'' and E'') Amplified view of the autopods in D' and E', respectively, marked by a dashed line box. The autopods are characterized by shortened skeletal elements and varied digit loss. (F) *LacZ* staining of the skull of the *Msx2^{cre/+}; R26R* reporter mice at E17.5, black arrow indicates Cre activity in skull. (G–G') Impaired intramembranous ossification and suture fusion (black arrowhead) in the skull of the *Msx2^{cre/+}; Wls^{c/c}* mutant was detected, in a comparison with the wild type. Abbreviations: FL, forelimb; HL, hindlimb.

and B'). Correspondingly, *Fgf10* expression was weaker in the distal mesenchyme of the mutant due to the impaired AER structure (Figs. 5C and C'). The regression of the AER structure may be due to impairment of AER-derived Wnt signaling because Wnt3/ β -catenin is necessary for normal AER function and maintenance (Barrow et al., 2003).

The regression of the AER also resulted in the down-regulation of *Shh* expression in the ZPA (Figs. 5D and D'), which is a major regulator of anterior–posterior (AP) polarity (Riddle et al., 1993). The down-regulated *Shh* activity was further confirmed by a restricted *Gli1* expression domain (data not shown), as *Gli1* is a putative target of hedgehog pathway. Based on previous work, the defect in the *Shh* expression pattern may be caused by disruption of the *Fgf/Gremlin/Shh* feedback loop (Verheyden and Sun, 2008). Concerning dorsal–ventral (DV) patterning, we detected expression of *Lmx1b* was expanded to ventral mesenchyme of the *Msx2^{cre/+}; Wls^{c/c}* mutant limb at E12.5 (arrow in Fig. 5 E' and Supplemental Fig. S6). However, no obvious difference in *Wnt7a* or *En1* expression between the mutant and the wild type limbs was found at E10.5 (data not shown), which are regarded as dorsal and ventral ectodermal signals respectively (Chen and Johnson, 2002). These data suggested that the ventralization of the mutant limb was progressive, being consistent with the phenotypes of the *Msx2^{cre/+}; Wnt3^{c/c}* mouse (Barrow et al., 2003). Taken together, the loss of ectodermal *Wls* directly or indirectly affects limb patterning in three directions.

Premature regression of undifferentiated distal mesenchyme without ectodermal *Wls*

The abnormal AER structure in the *Msx2^{cre/+}; Wls^{c/c}* mutant most likely affected the identity of the distal mesenchyme, thus disrupting limb outgrowth and structure. The *Sox9* expression domain was disorganized at E12.5 at the autopod level in the *Msx2^{cre/+}; Wls^{c/c}* mutant limb (Figs. 5F and F'), in agreement with the deformed autopod

skeletons. In addition, distal mesenchymal cells prematurely lost their progenitor identity, as demonstrated by significant reduction of *Msx1* and *Hoxd13* expression (Figs. 5G–H'). Expression of another distal mesenchyme marker, *Wnt5a*, was also greatly reduced (data not shown). Combined with the confined *Fgf10* expression at E10.5 (Figs. 5C and C'), the diminished expression of these progenitor markers suggests that the undifferentiated distal mesenchyme regresses quickly due to the loss of ectodermal Wnt signaling.

Altered cellular behaviors with the loss of mesenchymal or ectodermal *Wls*

Skeletal agenesis in the *Prx1^{cre/+}; Wls^{c/c}* and *Msx2^{cre/+}; Wls^{c/c}* mutants might result from either impaired cell proliferation, impaired cell survival or both during limb development. In *Prx1^{cre/+}; Wls^{c/c}* mutant limbs at E12.5, mesenchymal cell proliferation was reduced compared with controls (Figs. 6A and A'); so did in *Wnt5a* null mutant (data not shown). However, extensive cell death was not significantly detected in the mutant limb at E12.5 (Supplemental Figs. S3C and C'), when autopod had already appeared to be obviously shortened in the mutant. In addition, strong apoptosis began to emerge ubiquitously in the distal region of the mutant limb at E13.5, while it was only detected in the interdigital region of the normal limb at this time, as indicated by LysoTracker (Figs. 6B and B'), a dye specifically marking cells undergoing programmed cell death (PCD) (Vitelli et al., 2003). The increased cell death at this stage may be the consequence of AER regression. In the *Msx2^{cre/+}; Wls^{c/c}* mutant limb at E12.5, cell proliferation (measured by BrdU incorporation) was also decreased (Figs. 6C and C'), while cell death (labeled by TUNEL staining) was markedly increased in the distal limb mesenchyme (Figs. 6D and D'). Moreover, BrdU incorporation was much lower in the ventral mesenchyme than in its dorsal counterpart, most likely due to the stronger *Cre* activity in ventral ectoderm in *Msx2-Cre* mice (Figs. 6C and C'). Therefore, the reduction in cell proliferation accounted for

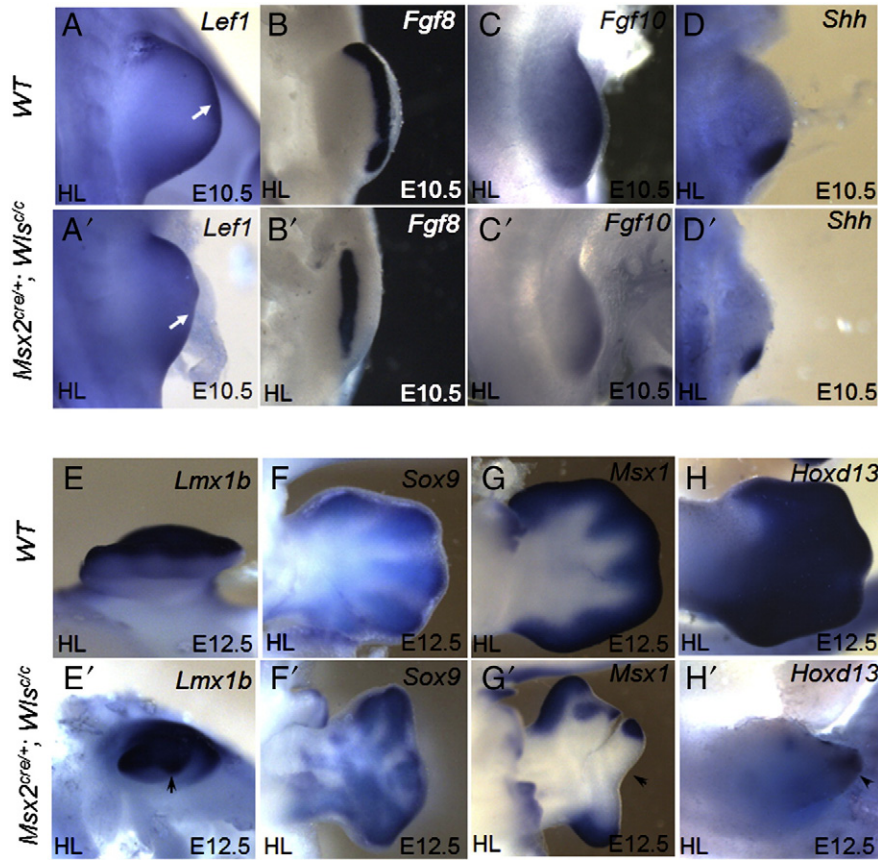


Fig. 5. Disrupted limb patterning with the absence of ectodermal *Wls*. (A and A') Canonical Wnt signaling activity, indicated by *Lef1* expression, is down-regulated in the distal limb of the *Msx2^{cre/+}; Wls^{c/c}* mutant (white arrows). (B and B') The AER, labeled by *Fgf8*, is thinner and narrower in the *Msx2^{cre/+}; Wls^{c/c}* mutant than in the wild type. (C and C') *Fgf10* expression in the distal mesenchyme is compromised with respect to wild type. (D and D') *Shh* expression is also confined to a much smaller region, thus affecting AP patterning. (E and E') *Lmx1b* is usually expressed in the limb dorsal mesenchyme, but its expression expands ventrally in the mutant limb at E12.5, as indicated by the black arrowhead. (F and F') *Sox9* expression is disorganized in the mutant autopod, which indicates disturbed digit patterning and formation. (G and G') The mutant distal mesenchyme is characterized by remarkably reduced *Msx1* expression, which even disappears in some regions (black arrow). (H and H') In a severely affected mutant, *Hoxd13* mRNA is almost lost in the distal mesenchyme, only a little expression remains in the most distal region (black arrowhead). Abbreviations: FL, forelimb; HL, hindlimb.

the defective distal limb structures in both the *Prx1^{cre/+}; Wls^{c/c}* and the *Msx2^{cre/+}; Wls^{c/c}* mutants, while increased cell death also contributed to the dysgenesis of *Msx2^{cre/+}; Wls^{c/c}* mutant. Taken together, these data suggest that ectodermal Wnts are indispensable for cell proliferation and survival of the distal mesenchyme, while mesenchymal Wnts are also essential for cell proliferation.

Defects in limb soft tissue formation in ectodermal Wls-depleted limb

In addition to the defects in limb PD patterning and skeletons of *Msx2^{cre/+}; Wls^{c/c}* mutant mice, there was also an obvious dysgenesis of limb soft tissues such as muscle, tendon/ligament and dermis, especially in the distal limb. All of these tissues display progressive

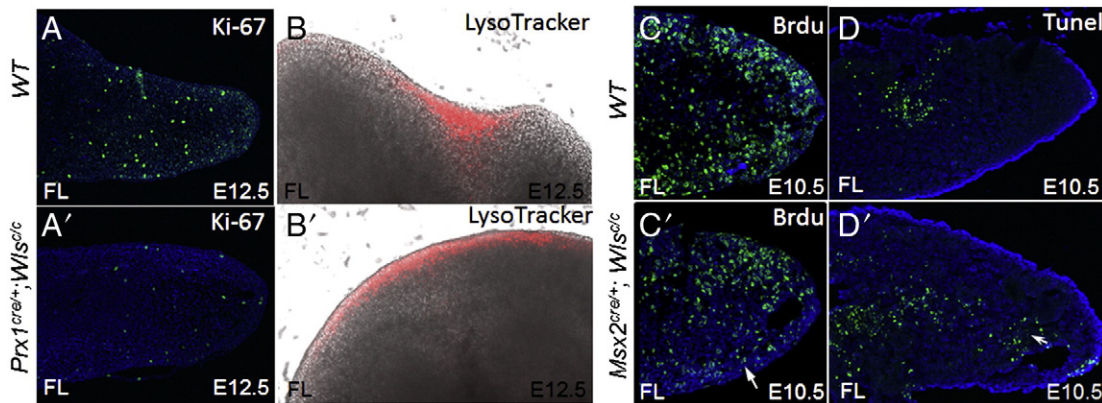


Fig. 6. Cell behavior in the distal limbs of *Prx1^{cre/+}; Wls^{c/c}* and *Msx2^{cre/+}; Wls^{c/c}* mutant embryos is changed. (A and A') Mesenchymal proliferation is decreased in the forelimb of *Prx1^{cre/+}; Wls^{c/c}* at E12.5, as indicated by Ki-67. (B and B') Cells in the undifferentiated mesenchymal ring of *Prx1^{cre/+}; Wls^{c/c}* at E13.5 undergo extensive apoptosis and are labeled by LysoTracker. (C and C') The proliferation in the distal mesenchyme is decreased, especially in the ventral half, in the *Msx2^{cre/+}; Wls^{c/c}* mutant forelimb at E10.5 (white arrow), as revealed by BrdU incorporation. (D and D') TUNEL results points to elevated apoptosis in the distal mesenchyme of the forelimb of *Msx2^{cre/+}; Wls^{c/c}* mice at E10.5 (white arrowhead). Abbreviations: FL, forelimb; HL, hindlimb.

defects from proximal to distal (Figs. 7A and A'). For instance, mature muscle fiber could be detected by Myosin antibody in the stylopod (green rectangle in Figs. 7A and A'), but not in the autopod, of the mutant limb at E17.5. In the distal zeugopod, the defects in the formation of soft tissues (Figs. 7C and C'), including muscle and tendon/ligament (red arrow in Figs. 7B and C) were very obvious in the mutant forelimb at E17.5. Meanwhile, dermis differentiation and hair follicle formation were also blocked, as reflected by K5 expression (Figs. 7B and B'). In the autopod of the *Msx2^{cre/+}; Wls^{c/c}* mutant, it was hard to detect any soft tissue, coupled with varied missing digits (Figs. 4D' and E'; 7A'). Comparatively, the defects were much more severe in the ventral limb than in dorsal limb (Figs. 7C and C'), which is probably due to stronger *Msx2-Cre* activity in ventral limb ectoderm.

Changes in molecular expression could also be detected corresponding to histological alteration. *Pax3* is expressed in the migrating myoblasts and usually serves as a good marker for myoblast migration (Buckingham et al., 2003). We found that in *Msx2^{cre/+}; Wls^{c/c}* limbs at E10.5, *Pax3* expression was decreased with respect to wild type (Figs. 8A–B'). The reduction was much more obvious in the hindlimb (arrows in Figs. 8B and B') than in the forelimb (arrows in Figs. 8A and A'). At E12.5, muscle differentiation was also impaired in the autopod without ectodermal *Wls*, as revealed by the muscle marker *Myogenin* (arrows in Figs. 8C and C'). In addition, tendon/ligament formation was also severely affected in the mutant limb at E12.5, as reflected by the loss of *Scleraxis* expression (arrows in Figs. 8D and D'), which is a marker for tendon/ligament progenitors (Murchison et al., 2007).

As the induction of distal tendon/ligament formation by ectodermal Wnt signaling was identified at the first time, we tested whether it was directly induced by canonical Wnts, which are mainly secreted by the ectoderm (Witte et al., 2009). We performed a luciferase reporter assay with various fragments of the *Scleraxis* promoter linked to the pGL3-Luc vector. The promoter region contains two presumptive Lef1/Tcf1 binding motifs, at –1156 to –1147 and at –742 to –733. The mutation of each presumptive Lef1/Tcf1 binding motif impaired the luciferase induction activity (Fig. 8E). The luciferase assay suggests that the *Scleraxis* promoter is strongly responsive to canonical Wnt stimulation.

Loss of mesenchymal β -catenin impaired soft tissue formation

Because we could not directly discern which Wnt pathway or ligand is responsible for the phenotypes in *Msx2^{cre/+}; Wls^{c/c}* limbs, we genetically modified the canonical Wnt pathway mediator, β -catenin, and dissected a hypomorphic β -catenin loss-of-function mutant, *Prx1^{Cre/+}; Catnby^{c/c}*. The β -catenin loss-of-function allele *Catnby^{c/c}* is floxed between exons 3 and 6, producing a null allele upon recombination by *Prx1-Cre* (Guo et al., 2004). The severe loss-of-function of β -catenin led to the disruption of limb PD and AP patterning (Fig. S5). The limb of the hypomorphic β -catenin mutant displayed various tissue defects, which were also observed in the *Msx2^{cre/+}; Wls^{c/c}* mutant (Fig. 9). These defects included loss of hair follicles and melanogenesis in the dorsal dermis of limb (Figs. 9B–C') as well as impaired tendon/ligament formation (arrows in Figs. 9D and D'). Consistent with the morphological defects, expression of the marker genes, *Dermo1* and *Scleraxis*, were reduced in the loss-of-function mutant (Figs. 9E–G').

Collectively, evidence from both the *Msx2^{cre/+}; Wls^{c/c}* and *Prx1^{Cre/+}; Catnby^{c/c}* mutants strongly implies that ectoderm-derived canonical Wnts are necessary for events during the morphogenesis of various mesenchyme-derived tissues, including myoblast migration and differentiation, distal tendon/ligament induction and dermis specification. By contrast, mesenchymal Wnts have minor morphological or molecular effects on the morphogenesis of these tissues (Supplemental Fig. S5A, A').

Discussion

Limb development has long served as an ideal model for patterning and morphogenesis. During limb development, most of the Wnt family members show dynamic and overlapping expression. Thus, it is promising to manipulate *Wls* as a new way to provide an overall view of Wnt function in limb development. Limb ectoderm or mesenchyme-specific deletion of *Wls* revealed some unexpected roles for Wnt signaling in limb patterning and morphogenesis, especially in coordinating distal soft tissue formation.

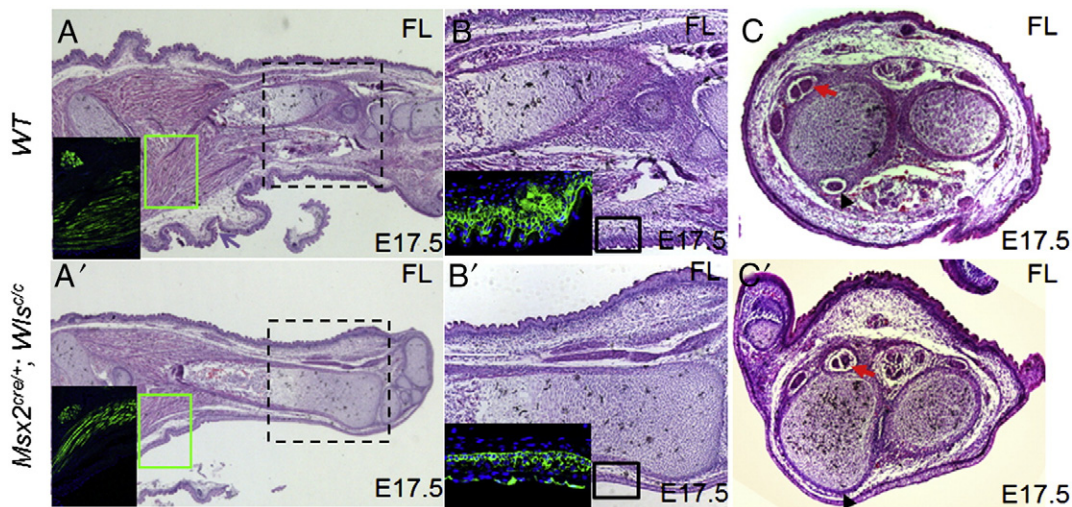


Fig. 7. Multiple tissue formation defects in the *Msx2^{cre/+}; Wls^{c/c}* mutant. (A and A') Sagittal overview of E17.5 forelimbs. The mutant forelimbs have reduced and malformed muscle mass in the stylopod. The muscle mass in the region of the green rectangle was immunostained by Myosin antibody and the result is displayed in the lower left corner. (B and B') Amplified view of distal zeugopods that correspond to the black dashed line rectangles in A and A'. Ventral tendon and muscle are indiscernible and ventral dermis is formed but significantly impaired in mutant, including loss of hair follicles and reduced expression of K5, a marker of the basal layer and hair follicle outer root sheath. (C and C') Transverse view of distal zeugopods. Dorsal tendon is present in both wild type and mutant (red arrow) but lost in the ventral part of mutant limb (black arrowhead). Abbreviation: FL, forelimb.

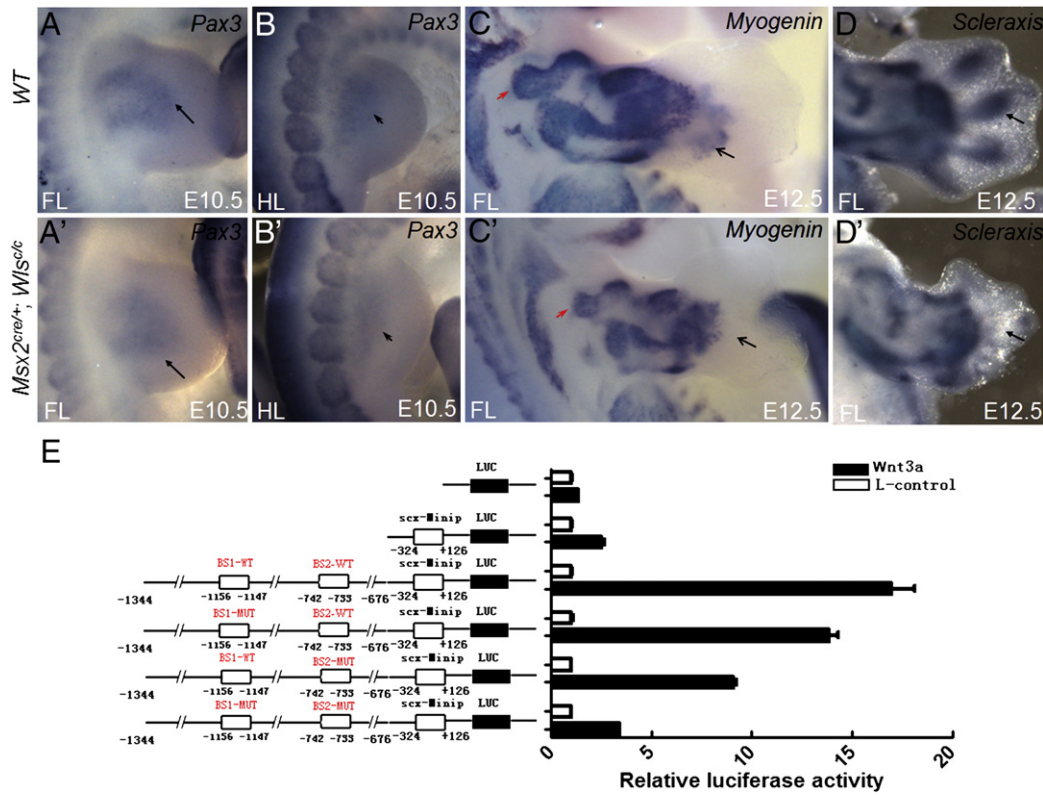


Fig. 8. Ectodermal *Wntless* is necessary for the development of distal limb muscle and tendons. (A–B') Myoblast migration from somite to limb, revealed by the decrease of *Pax3* expression, is impaired at E10.5. The reduction of *Pax3* expression is mild in the mutant forelimb (A and A', black arrows) but is remarkable in the hindlimb (B and B', black arrowheads). (C and C') Myoblast differentiation is also impaired in the autopod of forelimb, as revealed by the expression of *Myogenin* at E12.5 (red arrow heads and black arrows). (D and D') *Scleraxis* expression is lost in the mutant distal limb (black arrows). (E) The direct induction of tendon/ligament by Wnt/ β -catenin signaling is confirmed. The responsiveness of the *Scleraxis* promoter (-1344 to -676) to Wnt3a stimulation is analyzed using the luciferase reporter. Each mutation in the two presumptive Lef1/Tcf1 binding sites (-1156 to -1147; -742 to -733) impairs the responsiveness of this promoter to Wnt3a induction in an additive manner. Abbreviation: FL, forelimb.

Wls is required for the secretion of canonical and non-canonical Wnts in limb development

Wls has been reported to mediate the secretion of Wnt3a and Wnt5a in HEK293T cells (Banziger et al., 2006; Bartscherer et al., 2006). In mice, development of the body axis in a *Wls* null mutant is impaired due to the disruption of Wnt3 generation (Fu et al., 2009). *Wls* mediates both the production of xWnt4 in *Xenopus* and β -catenin-independent functions in *Planaria* (Adell et al., 2009; Kim et al., 2009). However, there is no strong evidence from mouse genetic analyses that *Wls* is required for the secretion of non-canonical Wnts. In addition, an *Evi/Wls* mutant in the fruit fly does not display the typical Wnt/PCP defects (Bartscherer et al., 2006). In our experiment, when *Wls* was depleted in the limb mesenchyme by *Prx1-Cre*, limb defects phenocopied those of the *Wnt5a*^{-/-} mutant (Fig. 2). During the preparation of this paper, another group showed that *Wls*-mediated Wnt5a secretion regulates angiogenesis (Stefater et al., 2011). These observations suggest that *Wls* is required for the secretion of Wnt5a protein *in vivo*.

In addition, similar phenotypes are observed between *Wls* knockout mutants and several canonical Wnt-deficient mice. For example, *Wls* total knockout mice have body axis defects that are similar to *Wnt3* null mice (Fu et al., 2009). Our *Msx2*^{cre/+}; *Wls*^{c/c} mice display a suture fusion defect in the skull, which is similar to what is observed in *Wnt9a*^{-/-} null embryos (Figs. 4G and G'), indicating an involvement of *Wls* in Wnt9a production (Spater et al., 2006). Taken together, these results suggest a requirement for *Wls* in the secretion of multiple Wnts, including canonical and non-canonical Wnt ligands, in limb development.

Ectodermal Wnts regulate limb patterning in different axes

Wnt signaling is reported to regulate limb patterning in three axes. In PD patterning, Wnt3/ β -catenin has been revealed to promote limb outgrowth by maintaining AER structure (Barrow et al., 2003). Recently, it was also found to synergize with *Fgfs* in maintaining distal identity of limb bud (ten Berge et al., 2008). The limb deformity in *Msx2*^{cre/+}; *Wls*^{c/c} mice, including skeletal element loss and diminished expression of *Fgf8* (Figs. 5B and B'; 5H and H'), resembled the mutant in *Wnt3* ectodermal inactivation (Barrow et al., 2003). After ablating Wnt3 or β -catenin in the ventral ectoderm by *Msx2-Cre* (Barrow et al., 2003), limb DV patterning is also progressively disrupted, as was observed in our *Msx2*^{cre/+}; *Wls*^{c/c} mutant (Figs. 5E and E'). On the other hand, the dorsal flexure and defective soft tissue formation in the limb autopod was distinct from the *Wnt3* ectodermal null mutant (Figs. 4B and B'). Therefore, we speculate that Wnt3 is the major ectodermal Wnt regulating limb PD patterning, while other ectodermal Wnts contribute to limb tissue specification.

In terms of limb DV and AP patterning, Wnt7a is a key Wnt protein that not only determines limb dorsal identity by inducing *Lmx1b* expression (Riddle et al., 1995), but also affects AP patterning by maintain *Shh* expression in the ZPA (Yang and Niswander, 1995); however, the signal cascades that are triggered by Wnt7a remain elusive (Chen and Johnson, 2002; Kengaku et al., 1998). In *Msx2*^{cre/+}; *Wls*^{c/c} mutant limbs, AP and DV patterning were also disrupted (Figs. 5 and Supplemental Fig. S4). However, we could not exclude a role for other ectodermal Wnts besides *Wnt7a* in regulating limb DV patterning.

The mesenchymal and ectodermal Wnts differentially regulate the pool of distal mesenchymal progenitors

The removal of ectodermal Wls lead to a distal defect of AER maintenance with premature regression of the distal mesenchyme, as shown by the swift loss of expression of progenitor markers and extensive apoptosis (Figs. 5G–H'; 6D and D'). This result is similar to the findings in *Msx2^{cre/+}; Wnt3^{c/c}* mice (Barrow et al., 2003) and suggested that the role of ectodermal Wnts is to sustain AER structure and maintain the undifferentiated pool of distal mesenchyme progenitors (Figs. 5 and 6C–D'). By contrast, the ablation of mesenchymal Wls prevented distal mesenchyme from differentiating even after AER regression (Fig. 3). Therefore, we speculate that the mesenchymal progenitors are maintained by ectodermal Wnts and repressed by mesenchymal Wnts. They differentially controls the mesenchymal differentiation, thus regulate the pool size of the distal mesenchymal progenitors. This speculation is in agreement with the notion that Wnt5a, the major mesenchymal Wnt, antagonizes and inhibits canonical Wnt signaling in distal limb mesenchyme (Gao et al., 2011; Topol et al., 2003). In other words, we identified mesenchymal Wnt as a negative regulator of distal limb mesenchyme identity, which exerts its function indirectly through antagonizing ectodermal canonical Wnts. It was independent of Fgf signaling because *Fgf8/Fgf10* expression was not altered in mesenchymal Wls null mutants (Supplemental Fig. S3).

Wls itself could play a role in mediating the feedback crosstalk between Wnts in the two germ layers. As reported previously, Wls is a direct transcriptional target of the canonical Wnt pathway (Fu et al., 2009). The ectodermal inactivation of Wls decreased the expression itself not only in the ectoderm but also in the underlying mesenchyme (Fig. S1D). The reduction of mesenchymal Wls feedback impaired Wnt secretion and function, contributing to the complex limb deformity in the ectodermal Wls null mutant. However, the

ectodermal inactivation of Wls presented much more severe phenotypic consequences than the mesenchymal Wls null mutant. These stronger phenotypes may have resulted from the additional AER defect and impaired Fgf signaling activity in the ectodermal null embryo (Figs. 5B–C').

Wnts regulate limb distal identity in a manner distinct from Fgf signaling

Based on the phenotypes of the mesenchymal and ectodermal Wls knockouts, Wnt proteins are more likely to regulate distal limb identity. The removal of ectodermal or mesenchymal Wls resulted in defects that were more severe in the distal than in the proximal skeleton. The defects observed in the ectodermal Wls null mutant could be ascribed to the combined effects of increased cell death, decreased cell proliferation and failure of soft tissue specification in the distal mesenchyme (Figs. 6C–D'; 7C and C'). The truncated limbs of the *Prx1^{cre/+}; Wls^{c/c}* mice could also be attributed to decreased mesenchymal cell proliferation (Figs. 7A and A'), so did for the phenotypes in the *Wnt5a* null mutants (Yamaguchi et al., 1999). Our observations suggest Wnts, especially ectodermal Wnts, regulate distal limb identity by promoting cell proliferation and cell survival and sustaining soft tissue morphogenesis.

AER-Fgf signaling has been widely recognized as the distal signal for limb patterning (Cooper et al., 2011). Fgfs and Wnts coordinately regulate distal limb mesenchyme differentiation (ten Berge et al., 2008). Yet based on our evidence, they have distinct ways of modulating distal limb development. Firstly, ectodermal Wnts act upstream of Fgf in maintaining AER structure. The ectodermal inactivation of Wls or *Wnt3* diminished *Fgf8* expression, thus confining the underlying *Fgf10* expression (Figs. 5B and B'; Barrow et al., 2003). Secondly, AER-Fgf signaling maintains cell survival in the proximal limb mesenchyme (Sun et al., 2002; Yu and Ornitz, 2008). By contrast, ectodermal Wnts sustain distal limb cell survival (Figs. 6D and D').

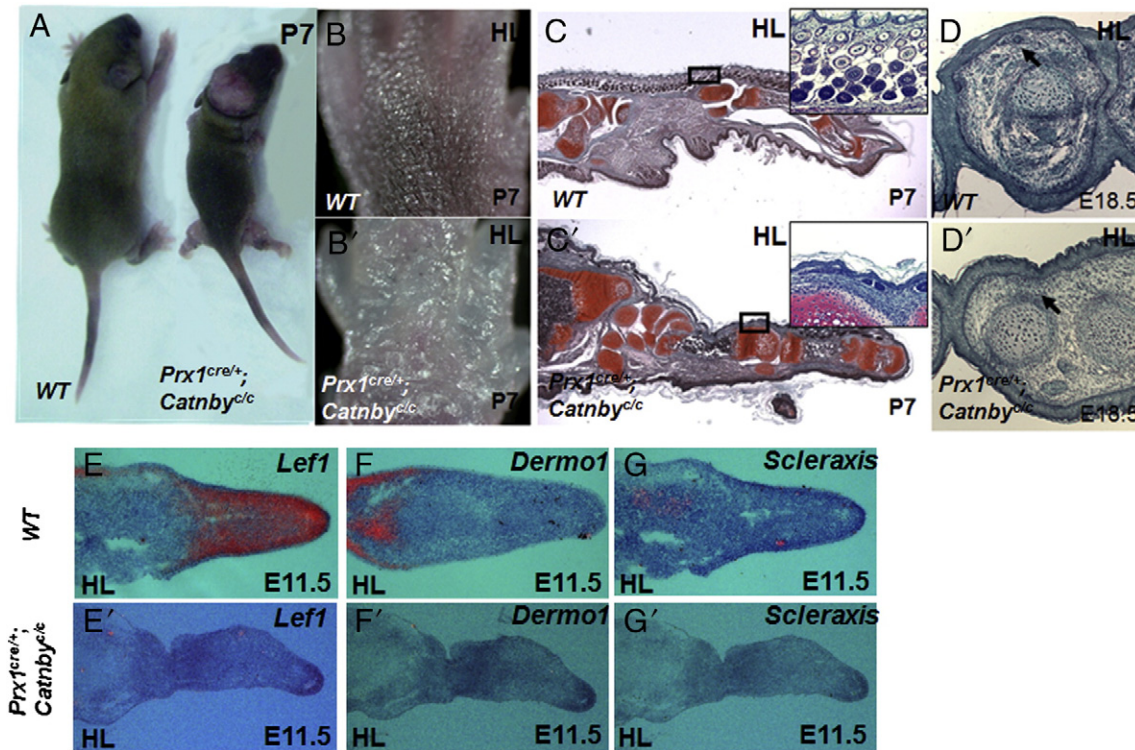


Fig. 9. Defective limb tissue formation in response to the inactivation of mesenchymal β -catenin. (A) Overview of the hypomorphic *Prx1^{Cre/+}; Catnby^{c/c}* mutant at P7. (B and B') Loss of hair in the mutant dorsal autopod dermis. (C and C') Hair follicle formation is impaired in the mutant limb at P7. A patch of skin with hair follicles is outlined in the box in the upper right corner. (D and D') Defective dorsal tendon/ligament formation (black arrow) is revealed by safranin O staining of the autopods in a transverse section at P7. (E and E') *Lef1* expression almost disappears in the mutant limb, indicating the removal of canonical Wnt activity by β -catenin knockout. (F–G') *Dermo1* (F and F') and *Scleraxis* (G and G') are not expressed in the distal limb of the mutant embryo at E11.5. Abbreviation: HL, hindlimb.

Furthermore, AER-Fgf alone is not necessary to sustain the proliferation of distal mesenchyme (Li et al., 2005). Conversely, both ectodermal and mesenchymal Wnts had positive roles for proliferation of the distal mesenchyme (Figs. 6A and A'; C and C').

Ectodermal Wnts are essential for multiple limb soft tissue morphogenesis

Following early limb patterning, limb morphogenesis is mainly referred to as the specification and organization of various limb tissues, such as skeletal elements, muscle, tendon/ligament and dermis. Wnts have been shown to guide the differentiation of various limb tissues. For instance, mesenchyme progenitors preferably differentiate into soft connective tissue under the effect of Wnt signaling (ten Berge et al., 2008); while ectodermal Wnt6 signaling induces myoblast migration and myogenesis through the activation of Pax3/Myf5 transcriptional factors in the chicken (Geetha-Loganathan et al., 2005). Our observations also demonstrate that ectodermal Wnt signaling plays multiple roles in organizing limb morphogenesis, including roles in myoblast migration and differentiation, tendon/ligament induction and dermis specification. The myocytes and muscle mass were remarkably diminished following the loss of ectodermal Wls or mesenchymal β -catenin, as revealed by immunostaining and histochemical analysis (Figs. 7 and 9). Our genetic data confirmed that ectodermal Wnts, possibly Wnt6, induced myoblast migration and myogenesis by a conserved mechanism. In addition, in null mutants of ectodermal Wls and mesenchymal β -catenin, dermis formation was also obviously inhibited (Figs. 7 and 9). It has been reported that canonical β -catenin signaling is absolutely required and sufficient for specification of dermal cells (Atit et al., 2006; Tran et al., 2011). Therefore, it is speculated that the ectodermal Wnts, especial canonical Wnts, instruct limb dermis formation.

Interestingly, tendon/ligament formation in the distal limb was first found to be affected by the removal of ectodermal Wls and mesenchymal β -catenin. Indeed, distal tendon formation was impaired to a much greater extent than proximal tendon formation, as evidenced by *Scleraxis* expression (Figs. 8D and D'). This difference may be due to the different developmental processes of these tendons. Proximal and distal tendons derive from common progenitors of the lateral plate mesoderm. However, proximal tendon formation is tightly coupled with myogenesis, whereas the distal tendon develops independently from a mesenchymal lamina underlying the ectoderm, and its development is coordinated with skeletal formation (Liu et al., 2010). Although ectodermal signal is supposed to induce distal tendon formation, the pathway that plays this inductive role has not been clarified (Schweitzer et al., 2010). Our data strongly suggest ectodermal Wnt/ β -catenin signaling directly induces distal tendon formation, as evidenced by the finding that the *Scleraxis* promoter luciferase construct displayed obvious responsiveness to Wnt3a induction. However, since there are also severe skeletal defects in the autopod, we could not absolutely exclude that the tendon loss is secondary to skeletal deformity. By contrast, mesenchymal Wnts display no significant effect in limb tissue-specific differentiation (Supplemental Fig. S5). In summary, our results demonstrate that ectodermal and mesenchymal Wnts differentially regulate the limb mesenchymal differentiation. Ectodermal Wnt signaling centrally organizes limb morphogenesis, including myogenesis, dermal specification and distal tendon/ligament formation.

Supplementary materials related to this article can be found online at doi:10.1016/j.ydbio.2012.02.019.

Acknowledgments

We thank Dr. Mark Lewandoski of the NIH/NCI for providing us with the *Msx2-Cre* mice. This work was supported by the National Major Fundamental Research 973 program of China under grant

(2007CB947301 and 2012CB966903) and by grants from the National Natural Science Foundation of China (31171396 and 31100624) and Pujiang Talent (08PJ1407200).

References

- Aberle, H., et al., 1996. Cadherin-catenin complex: protein interactions and their implications for cadherin function. *J. Cell. Biochem.* 61, 514–523.
- Adell, T., et al., 2009. Smed-Evi/Wntless is required for beta-catenin-dependent and -independent processes during planarian regeneration. *Development* 136, 905–910.
- Atit, R., et al., 2006. Beta-catenin activation is necessary and sufficient to specify the dorsal dermal fate in the mouse. *Dev. Biol.* 296, 164–176.
- Banziger, C., et al., 2006. Wntless, a conserved membrane protein dedicated to the secretion of Wnt proteins from signaling cells. *Cell* 125, 509–522.
- Barrow, J.R., et al., 2003. Ectodermal Wnt3/beta-catenin signaling is required for the establishment and maintenance of the apical ectodermal ridge. *Genes Dev.* 17, 394–409.
- Bartscherer, K., et al., 2006. Secretion of Wnt ligands requires Evi, a conserved transmembrane protein. *Cell* 125, 523–533.
- Bejsovec, A., 2000. Wnt signaling: an embarrassment of receptors. *Curr. Biol.* 10, R919–R922.
- Buckingham, M., et al., 2003. The formation of skeletal muscle: from somite to limb. *J. Anat.* 202, 59–68.
- Chen, H., Johnson, R.L., 2002. Interactions between dorsal-ventral patterning genes *lmx1b*, *engrailed-1* and *wnt-7a* in the vertebrate limb. *Int. J. Dev. Biol.* 46, 937–941.
- Cooper, K.L., et al., 2011. Initiation of proximal-distal patterning in the vertebrate limb by signals and growth. *Science* 332, 1083–1086.
- Fu, J., et al., 2009. Reciprocal regulation of Wnt and *Gpr177*/mouse *Wntless* is required for embryonic axis formation. *Proc. Natl. Acad. Sci. U. S. A.* 106, 18598–18603.
- Fu, J., H.M., Ivy Yu, et al., 2011. *Gpr177*/mouse *Wntless* is essential for Wnt-mediated craniofacial and brain development. *Dev. Dyn.* 240, 365–371.
- Gao, B., et al., 2011. Wnt signaling gradients establish planar cell polarity by inducing *Vangl2* phosphorylation through *Ror2*. *Dev. Cell* 20, 163–176.
- Geetha-Loganathan, P., et al., 2005. Ectodermal Wnt-6 promotes Myf5-dependent avian limb myogenesis. *Dev. Biol.* 288, 221–233.
- Guo, X., et al., 2004. Wnt/beta-catenin signaling is sufficient and necessary for synovial joint formation. *Genes Dev.* 18, 2404–2417.
- Hamburger, V., Hamilton, H.L., 1951. A series of normal stages in the development of the chick embryo. *J. Morphol.* 88, 49–92.
- Hill, T.P., et al., 2006. Multiple roles of mesenchymal beta-catenin during murine limb patterning. *Development* 133, 1219–1229.
- Kawakami, Y., et al., 2001. WNT signals control FGF-dependent limb initiation and AER induction in the chick embryo. *Cell* 104, 891–900.
- Kengaku, M., et al., 1998. Distinct WNT pathways regulating AER formation and dorsoventral polarity in the chick limb bud. *Science* 280, 1274–1277.
- Kim, H., et al., 2009. *Xenopus* *Wntless* and the retromer complex cooperate to regulate *XWnt4* secretion. *Mol. Cell. Biol.* 29, 2118–2128.
- Li, C., et al., 2005. *FGFR1* function at the earliest stages of mouse limb development plays an indispensable role in subsequent autopod morphogenesis. *Development* 132, 4755–4764.
- Liu, W., et al., 2010. The atypical homeodomain transcription factor *Mohawk* controls tendon morphogenesis. *Mol. Cell. Biol.* 30, 4797–4807.
- Logan, M., et al., 2002. Expression of *Cre* Recombinase in the developing mouse limb bud driven by a *Prlx* enhancer. *Genesis* 33, 77–80.
- Mariani, F.V., Martin, G.R., 2003. Deciphering skeletal patterning: clues from the limb. *Nature* 423, 319–325.
- Mariani, F.V., et al., 2008. Genetic evidence that FGFs have an instructive role in limb proximal-distal patterning. *Nature* 453, 401–405.
- Murchison, N.D., et al., 2007. Regulation of tendon differentiation by *scleraxis* distinguishes force-transmitting tendons from muscle-anchoring tendons. *Development* 134, 2697–2708.
- Port, F., et al., 2008. *Wingless* secretion promotes and requires retromer-dependent cycling of *Wntless*. *Nat. Cell Biol.* 10, 178–185.
- Riddle, R.D., et al., 1993. *Sonic hedgehog* mediates the polarizing activity of the ZPA. *Cell* 75, 1401–1416.
- Riddle, R.D., et al., 1995. Induction of the LIM homeobox gene *Lmx1* by *WNT7a* establishes dorsoventral pattern in the vertebrate limb. *Cell* 83, 631–640.
- Rosello-Diez, A., et al., 2011. Diffusible signals, not autonomous mechanisms, determine the main proximodistal limb subdivision. *Science* 332, 1086–1088.
- Scherz, P.J., et al., 2004. The limb bud *Shh-Fgf* feedback loop is terminated by expansion of former ZPA cells. *Science* 305, 396–399.
- Schweitzer, R., et al., 2010. Connecting muscles to tendons: tendons and musculoskeletal development in flies and vertebrates. *Development* 137, 2807–2817.
- Spater, D., et al., 2006. *Wnt9a* signaling is required for joint integrity and regulation of *Ihh* during chondrogenesis. *Development* 133, 3039–3049.
- Stefater III, J.A., et al., 2011. Regulation of angiogenesis by a non-canonical Wnt-Flt1 pathway in myeloid cells. *Nature* 474, 511–515.
- Sun, X., et al., 2002. Functions of FGF signalling from the apical ectodermal ridge in limb development. *Nature* 418, 501–508.
- ten Berge, D., et al., 2008. Wnt and FGF signals interact to coordinate growth with cell fate specification during limb development. *Development* 135, 3247–3257.
- Topol, L., et al., 2003. *Wnt-5a* inhibits the canonical Wnt pathway by promoting GSK-3-independent beta-catenin degradation. *J. Cell Biol.* 162, 899–908.

- Tran, T.H., et al., 2011. Role of canonical Wnt signaling/ β -catenin via Dermo1 in cranial dermal cell development. *Development* 137, 3973–3984.
- Verheyden, J.M., Sun, X., 2008. An Fgf/Gremlin inhibitory feedback loop triggers termination of limb bud outgrowth. *Nature* 454, 638–641.
- Vitelli, F., et al., 2003. TBX1 is required for inner ear morphogenesis. *Hum. Mol. Genet.* 12, 2041–2048.
- Witte, F., et al., 2009. Comprehensive expression analysis of all Wnt genes and their major secreted antagonists during mouse limb development and cartilage differentiation. *Gene Expr. Patterns* 9, 215–223.
- Yamaguchi, T.P., et al., 1999. A Wnt5a pathway underlies outgrowth of multiple structures in the vertebrate embryo. *Development* 126, 1211–1223.
- Yang, Y., Niswander, L., 1995. Interaction between the signaling molecules WNT7a and SHH during vertebrate limb development: dorsal signals regulate anteroposterior patterning. *Cell* 80, 939–947.
- Yu, K., Ornitz, D.M., 2008. FGF signaling regulates mesenchymal differentiation and skeletal patterning along the limb bud proximodistal axis. *Development* 135, 483–491.
- Yu, H.M., et al., 2010. Expression of Gpr177, a Wnt trafficking regulator, in mouse embryogenesis. *Dev. Dyn.* 239, 2102–2109.